Meteoritics & Planetary Science 42, Nr 11, 1995–2012 (2008)
Abstract available online at http://meteoritics.org

Coupled effects of impact and orogeny: Is the marine Lockne crater, Sweden, pristine?

T. KENKMANN[1*], F. KIEBACH[2], M. ROSENAU[3], U. RASCHKE[2], A. PIGOWSKE[2], K. MITTELHAUS[2], and D. EUE[2]

[1]Museum of Natural History—Mineralogy, Humboldt University Berlin, Invalidenstrasse 43, D-10115 Berlin, Germany
[2]Institute of Geosciences, Free University Berlin, Malteserstrasse 74–100, Berlin, Germany
[3]Department of Geodynamics, GeoForschungs Zentrum Potsdam, Telegrafenberg, 14473 Potsdam, Germany
*Corresponding author. E-mail: thomas.kenkmann@museum.hu-berlin.de

(Received 31 October 2006; revision accepted 13 May 2007)

Abstract–Our current understanding of marine-impact cratering processes is partly inferred from the geological structure of the Lockne crater. We present results of a mapping campaign and structural data indicating that this crater is not pristine. In the western part of the crater, pre-impact, impact, and post-impact rocks are incorporated in Caledonian thrust slices and are subjected to folding and faulting. A nappe outlier in the central crater depression is a relic of the Caledonian nappe cover that reached a thickness of more than 5 km. The overthrusted crater is gently deformed. Strike of strata and trend of fold axes deviate from standard Caledonian directions (northeast-southwest). Radially oriented crater depressions, which were previously regarded as marine resurge gullies formed when resurging seawater erosively cut through the crater brim, are interpreted to be open synclines in which resurge deposits were better preserved.

The presence of the impact structure influenced orogenesis due to morphological and lithological anomalies of the crater: i) a raised crater brim zone acted as an obstacle during nappe propagation, (ii) the occurrence of a central crater depression caused downward sagging of nappes, and (iii) the lack of an appropriate detachment horizon (alum shale) within the crater led to an enhanced mechanical coupling and internal deformation of the nappe and the overthrusted foreland. Preliminary results of 3-D–analogue experiments suggest that a circular high-friction zone representing the crater locally hinders nappe propagation and initiates a circumferentially striking ramp fault that delineates the crater. Crustal shortening is also partitioned into the crater basement and decreases laterally outward. Deformation of the foreland affected the geometry of the detachment and could be associated with the activation of a deeper detachment horizon beneath the crater. Strain gradients both vertically and horizontally result in non-plane strain deformation in the vicinity of the crater. The strain tensors in the hanging and foot walls may deviate up to 90° from each other and rotated by up to 45° with respect to the standard regional orientation. The observed deflection of strata and fold axes within the Lockne crater area as revealed by field mapping is in agreement with the pattern of strain partitioning shown in the analogue models.

INTRODUCTION

The number of meteorite impact craters discovered on Earth so far is relatively small (175; Earth Impact Database 2007) compared to other planets or satellites like the Moon. This can be attributed to a number of circumstances: i) two-thirds of the Earth's surface is covered by water, which hinders the discovery of submarine craters (the latter should be rare because of the young age of the oceanic crust and shielding by the water column [Shuvalov et al. 2005]); ii) craters on land are better accessible, but they are often subjected to either erosion or burial (Grieve 1991); and (iii) subduction of crater-bearing oceanic crust or incorporation of cratered continental crust into mountain-building processes cause deformation of impact craters and may ultimately lead to their complete destruction. If craters are affected by orogeny, proof of an impact origin becomes complicated because the initial crater geometry is usually destroyed. Breccias and pseudotachylites can form during both mountain-building and impact-crater formation. In such

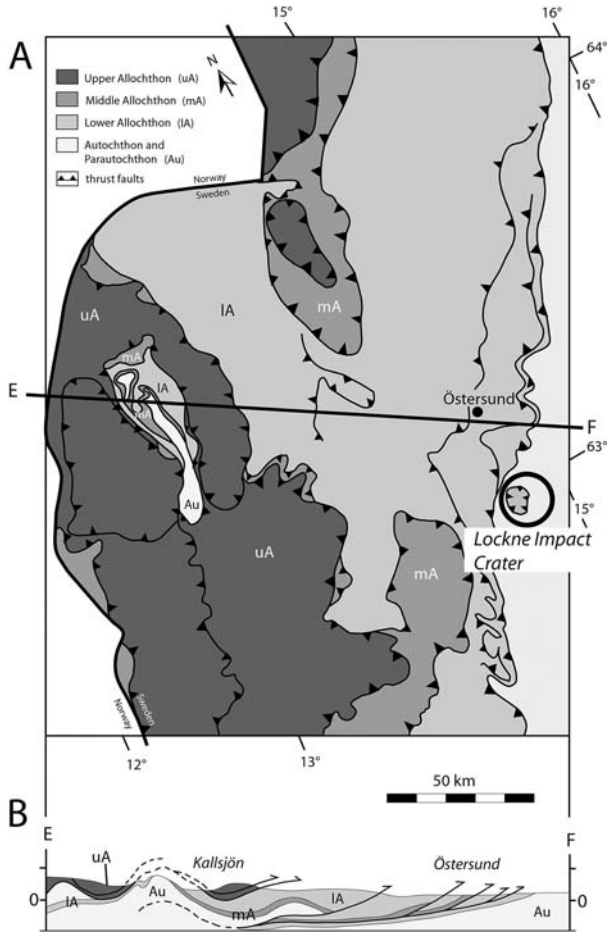

Fig. 1. a) Simplified tectonic map of the Caledonides of central Sweden (after Gee and Kumpulainen [1980]). The Lockne crater is situated at the eastern border of the Caledonian orogeny. b) Simplified east-west cross section through the Caledonian orogeny (after Gee and Kumpulainen [1980]).

cases, shock indicators like shatter cones, planar deformation features (PDFs), diaplectic glasses, and high-pressure phases (e.g., Langenhorst and Deutsch 1994; Stöffler and Langenhorst 1994; Kenkmann et al. 2005) are indispensable in proving the existence of a deformed crater.

There are a few examples of terrestrial impact craters that were affected but not destroyed by orogeny: Sudbury, Canada, (e.g., Riller 2005), Charlevoix, Canada (e.g., Trepmann and Spray 2005), Gardnos, Norway (French et al. 1997), and Lockne, Sweden, (e.g., Lindström et al. 1996; Sturkell 1998a; Lindström et al. 2005a). Here, we focus on the Lockne crater, which is situated at the eastern border of the Caledonian orogen in central Sweden (Fig. 1). Except for a general tilt of the structure by less than 1° to the northwest, this crater is regarded as virtually unaffected by orogeny (e.g., von Dalwigk and Ormö 2001; Lindström et al. 2005a). However, the present border of the Caledonides is the result of later erosion. The original thrust front was probably located more than 40 km further to the east, and the crater was buried by a pile of thrusts at least 5 km thick (Sturkell et al. 1998). A very efficient detachment horizon, the so-called Cambrian alum shale was used as the major thrust plane. It acted as a lubricant during nappe propagation and was an ideal mechanical decoupling horizon between the orogenic wedge and autochthonous foreland.

This study investigates the role of the post-impact Caledonian deformation onto the Lockne crater. As this crater becomes increasingly important as a reference for marine-cratering processes and is used as a standard for comparison with other "wet target" craters on Earth and Mars, a thorough and quantitative understanding of the post-impact history of this crater and a reconstruction of the crater's initial morphology is necessary. For this purpose, a geological mapping campaign was conducted within the framework of master's thesis work. The mapping concentrated on the western part of the Lockne crater, (west of Lake Locknesjön) with a particular focus on the analysis and quantification of deformation overprint. The subtraction of Caledonian deformation and restoration of the crater's initial shape is a future goal. To evaluate the control of the impact on thrusting and nappe movement, a further objective was to study impact-induced effects, i.e., modification of basement morphology and sedimentary cover sequence, on nappe propagation and orogenic architecture.

Geology of the Lockne Crater

The Lockne crater in Central Sweden (14°40′E, 63°00′N) formed in mid-Ordovician times (455 Ma) at the western continental shelf of the Baltic Shield (e.g., Lindström et al. 1996; Sturkell 1998a). The structure was discovered by Wickman (1988) who interpreted the origin of unusual breccias of the Lockne region as the products of an impact cratering process in a shallow sea. Lindstrom et al. (1991) refined the crater location. The discovery of PDFs in quartz grains from resurge deposits (Therriault and Lindström 1995) and its Ir enrichment (Sturkell 1998b) proved the impact.

The sub-circular Lockne crater has a subdued morphological expression due to the preferred erosion of sedimentary strata in its center and the presence of a crystalline brim up to 70 m high. The eastern half of the crater is covered by Lake Locknesjön and tills related to Quaternary glaciation. The central crater depression is 7 km in diameter and was excavated into crystalline basement. Gravity modeling as well as drill cores (Lindström et al. 1996) imply a weak uplift. The crater is surrounded by an elevated crater brim with brecciated and fractured crystalline rock that is interpreted as an overturned ejecta flap (Lindström et al. 2005a). Bore holes and exposures show that this brim is rootless and is underlain by Cambrian alum shale (Lindström et al. 2005a). The sediments surrounding this inner crater were locally stripped from the sub-Cambrian peneplain by the expanding water crater. The inner crater is partly covered by a nappe outlier of

the Caledonides. Resurge deposits are preserved inside and outside of the Lockne crater. Their presence suggests a water depth that was at least sufficient to overcome the brim wall (von Dalwigk and Ormö 2001).

Marine-target craters differ from craters formed on land (Ormö and Lindström 2000; Gersonde et al. 2002). The investigation of the Lockne structure has considerably contributed to our present knowledge of impact into wet environments and is regarded as a reference crater for marine impacts in which the projectile diameter has a similar size as the water depth (Ormö et al. 2002; Shuvalov et al. 2005). However, estimates of water depth at the time of impact range from 200 m (von Dalwigk and Ormö 2001) to 1000 m (Lindström et al. 1996). Recent numerical simulations of the impact (Shuvalov et al. 2005; Lindström et al. 2005b) achieved a best match between nature and modeling for water depths of 500–800 m.

The present relief of the crystalline basement shows several topographical lows along the crystalline brim in which resurge deposits are preserved. Lindström et al. (1996) and von Dalwigk and Ormö (2001) identified four such lows cutting through the brim in the southeast, southwest, northwest, and northeast directions (Fig. 2). The southeastern crystalline low in the Bergböle region ("Bergböle gully;" Fig. 2) is estimated to be ~1000 m wide and 100 m deep; the southwestern low in the Tandsbyn area ("Tandsbyn gully;" Fig. 2) is believed to be 50 m deep, 500–1000 m wide, and at least 2 km long. Recently, Lindström et al. (2005a) described another low in the south-southwest sector of the crater brim ("Långmyren gully"). Lindström et al. (1996) and von Dalwigk and Ormö (2001) interpreted these topographical lows as primary impact-related features and designated them as "resurge gullies." According to these authors and to Ormö and Miyamoto (2002) resurge gullies might have originated during ejection, but were enlarged by resurging seawater. In this study, it is suggested that the present topographic lows of the crater brim are not primary features, but were caused by gentle folding and down-faulting after the impact.

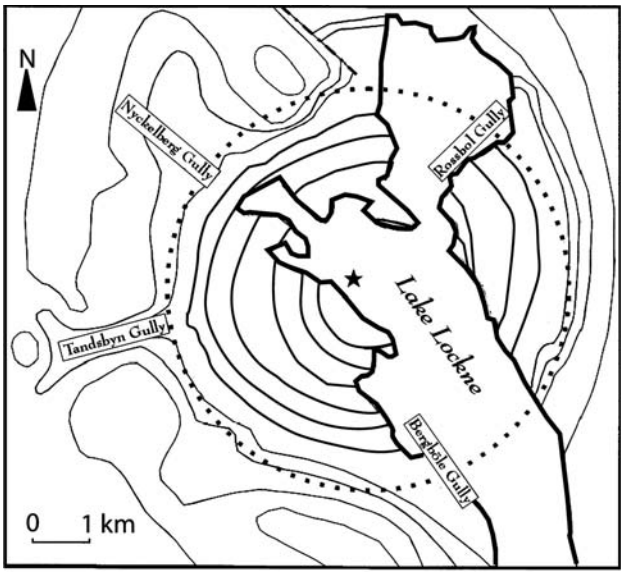

Fig. 2. Present relief of the crystalline surface of the Lockne crater as constructed by von Dalwigk and Ormö (2001). The crystalline brim shows topographical lows in its northwest, southwest, southeast, and northeast sectors that were interpreted as resurge gullies. Image after von Dalwigk and Ormö 2001.

Lockne Crater and the Caledonides

The crater is situated at the present Caledonian thrust front (Fig. 1). The eastern border of the Scandinavian Caledonides is a result of erosion. The nappes by far exceeded the thickness of the present remains within the center and west of the crater as illite crystallinity and organic maturation data indicate (Lundqvist and Andréasson 1987). A lower limit of overburden of the Lockne area has been estimated from fluid inclusion studies. Sturkell et al. (1998) measured average homogenization temperatures of fluid inclusions of 150 °C suggesting pressures of ~1.3 kbar that correspond to a burial of ~5 km. The crystallinity index of the alum shale and conodont alteration index as well as the presence of laumontite give an upper pressure and temperature boundary of 3 kbar and 300 °C, respectively, corresponding to a Caledonian burial of about 10 km. A burial of 5–10 km is in accordance with petrophysical modeling of the Caledonian foreland basin in the Jämtland area, which is modeled as a basin 7 km deep and 150 km wide (Middleton et al. 1996; Larson et al. 1999). Using average topographic slope and décollement angles derived for the Scandinaviean Caledonides (Warr et al. 1996), it is suggested that the frontal thrusts of the Caledonides might have reached 40–80 km farther to the east in the Lockne area. It is the late exhumation of the crater that caused the good preservation of the structure.

The Scandinavian Caledonides are dominated by a variety of nappes, collectively grouped into Lower, Middle, Upper, and Uppermost Allochthon (Roberts and Gee 1985; Gee et al. 1985) (Fig. 1). During the Caledonian orogeny (Silurian-Devonian), these units thrusted eastward over the Baltoscandian Platform, which consisted of Precambrian crystalline basement with a thin veneer of Early Paleozoic cover sediments (Gee and Kumpulainen 1980). Throughout much of the Caledonian front in Scandinavia, the Cambrian alum shale provides an ideal detachment surface above the Precambrian crystalline basement. Thus, the Precambrian crystalline basement is passive and virtually undeformed beneath the Caledonian front décollement, but is increasingly affected by Caledonian deformation further west (Roberts and Gee 1985). The amount of crystalline basement involved in the frontal nappes is very small and restricted to isolated slices. The Lower Allochthon and Parautochthon are largely composed of Early Paleozoic sediments (Jämtland supergroup) that detached, folded, and translated over the sole thrust at the alum shale level (Fig. 1).

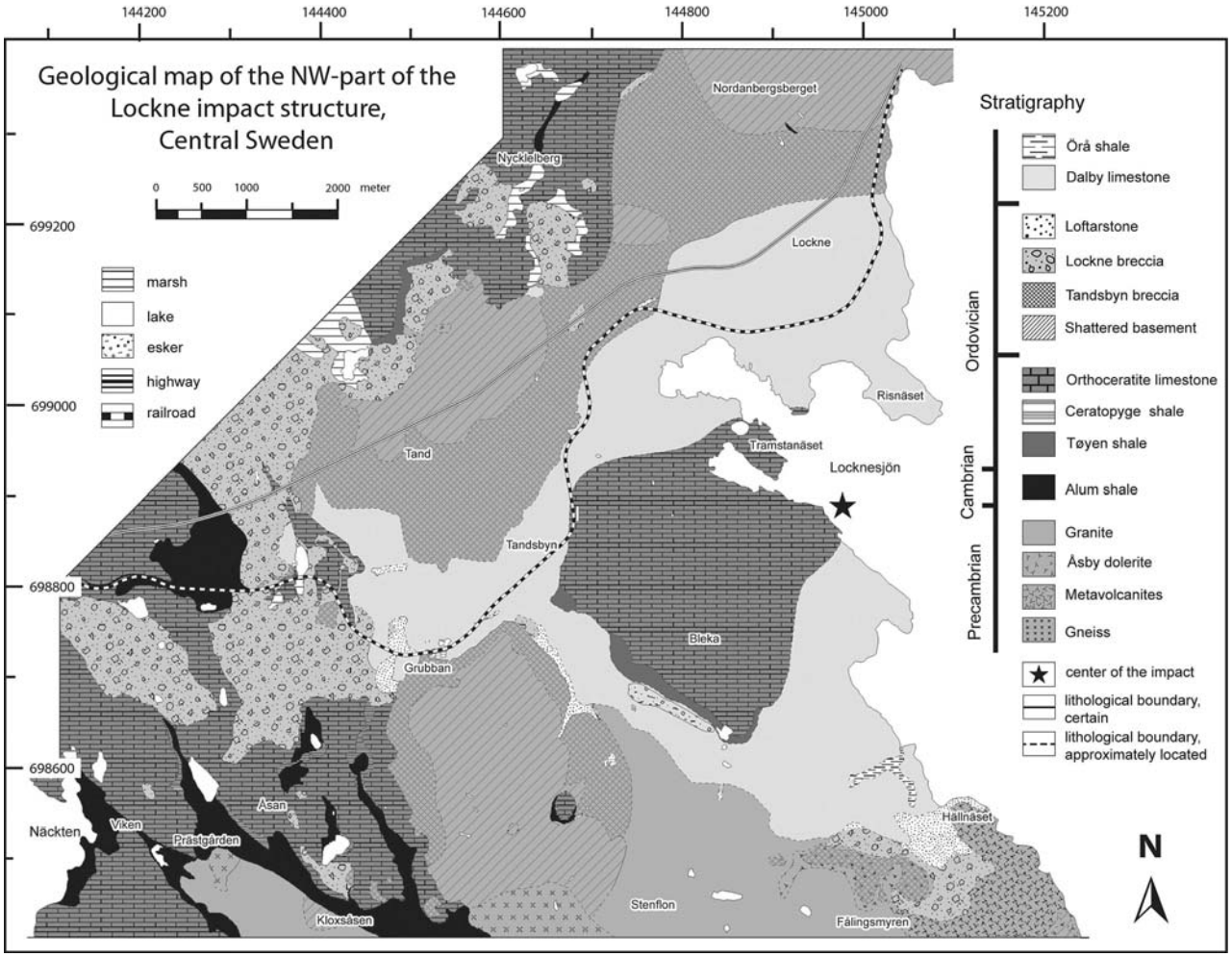

Fig. 3. GPS/GIS based geological map of the western part of the Lockne impact structure, central Sweden. Coordinates refer to the Swedish National grid. Mapping was conducted in 2005 in the framework of master's thesis work at Free University Berlin. See text for discussion.

In 1940, Thorslund had observed the lack of alum shale and irregular basement topography in the area of Lockne, although he was unaware of the presence of an impact crater. He described a basement high that rises up to 70 m above the floor of the surrounding peneplain and that is directly overlain by Ordovician limestones (Thorslund 1940). While the relationship to this "Lockne high" remained unclear, he identified three subordinate thrust units as specialties of the Lockne region. Sturkell and Lindström (2004), who reconstructed the topography of the sub-Cambrian peneplain and thereby the prominent alum shale detachment, also noticed irregularities in the Lockne area, without considering a causal context with the crater.

The deformation of the sub-Cambrian peneplain including the alum shale detachment, the presence of nappe relics, and the occurrences of topographic lows in the crater brim motivated us to examine the post-impact deformation on the Lockne crater in more detail and to assess the influence of the Lockne crater on nappe propagation during Caledonian orogeny. For the investigation we have chosen a combined approach of field analysis (Pigowske et al. 2006; Kenkmann et al. 2006) and analogue modeling.

METHODS

Geological mapping has focused on the western part of the Lockne crater (west of Lake Locknesjön) and comprises a total area of ~70 km^2 (Figs. 3–5). Standard geological mapping techniques were applied, including the use of GPS. The map was processed at a scale of 1:10,000 utilizing ArcGIS 8.01 software. Geological information is allocated to different layers, enabling the user to specify separate or common visualization of geologic information (Figs. 3–5). Structural analysis included the measurement of the dip of bedding, fault and cleavage planes, fault-slip vectors (striae and grooves), and trend of fold axes. For construction of the alum shale detachment surface, we applied the kriging grid interpolation method of the Surfer_8 software (Golden Software Ltd).

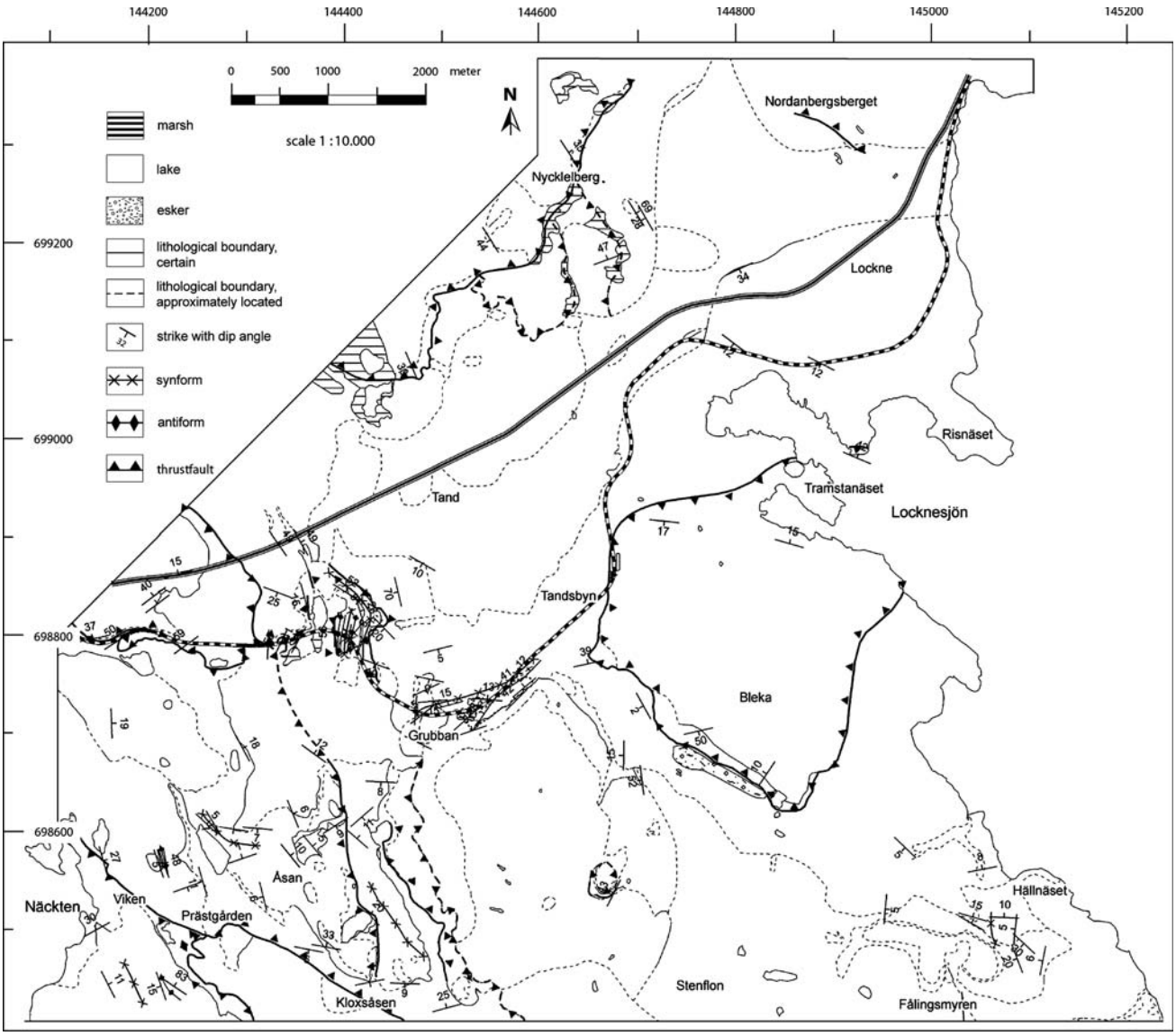

Fig. 4. Structural features of the studied region. Please note the Caledonian nappe system in the western part, the central nappe outlier, and the radial syncline in the western part of the crater (Tandsbyn area).

Polished cuttings and thin sections were prepared from various lithologies perpendicular to strata strike. For evaluating tilting of post-impact strata, it was critical to analyze sedimentary structures of post-impact sediments (Dalby limestone): we used Orthoceratite conches that were partly filled with marly sediment as geopetal markers. Cavities capped by the conches were later filled with sparite calcite cement. The transition from the sedimentary infill of the conches to the sparite cement defines a sub-horizontal plane at the time of deposition. The angles between bedding planes and geopetal markers were determined from photographs. The application of an image analysis package (Q-Win by Leica) enabled us to quantify the preferred orientation of sedimentary fabrics with respect to a bedding plane.

In order to understand how the crater was deformed by the Caledonian nappes, three-dimensional analogue "sandbox" experiments scaled for density and cohesion were conducted at the geodynamic laboratory of the GFZ-Potsdam. We investigated the effect of a crater as a circular frictional heterogeneity on the kinematical evolution of a fold-and-thrust belt. Such sandbox experiments have been widely applied to study the behavior of friction-controlled fold-and-thrust belts and accretionary wedges of convergent margins, which are considered to be analogous to wedges of sand or snow forming in front of a moving bulldozer, a concept known as the "critical wedge" or "critical taper" theory (e.g., Davis et al. 1983; Mulugeta 1988; Willett 1992; Liu and Ranalli 1992; Koyi 1997; Lohrmann et al. 2003; Hampel et al. 2004). According to this theory, the geometry, kinematics, and stress regime of an accretionary

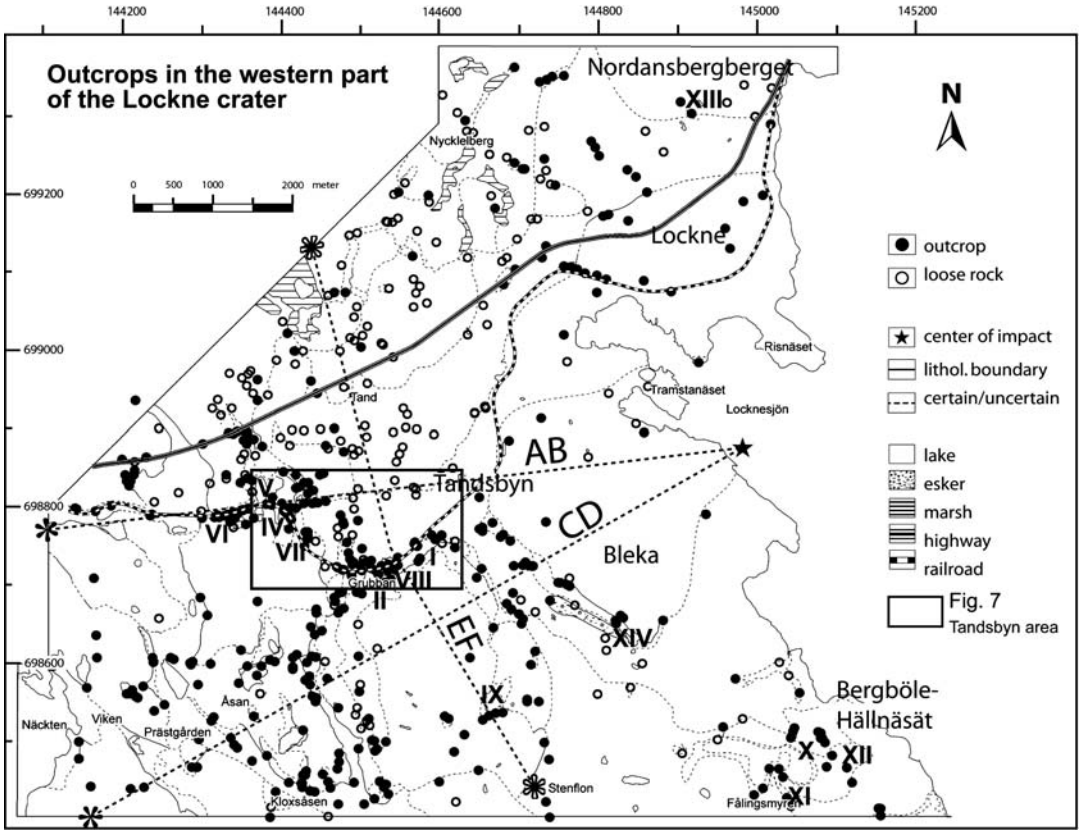

Fig. 5. Location of outcrops in the western Lockne area. Roman numbers refer to outcrops that are mentioned in the text. The rectangle gives the position of Fig. 7. AB, CD, and EF refer to the geological cross sections of Fig. 6.

wedge is controlled by only three factors: cohesion, internal, and basal shear strength. To adjust its geometry to the controlling parameters, the wedge may deform internally by diffuse deformation and/or faulting. When the wedge approaches the stable geometry, it is said to be in the critical stage, which means that no further internal deformation is required and the wedge may grow in a self-similar manner by frontal accretion equivalent to propagating fold-and-thrust belts in nature. Accordingly, a strong wedge (i.e., high friction) will develop a large taper and low aspect ratio of thrust sheets, whereas a weak wedge (i.e., low friction) will evolve to a narrow taper with high aspect-ratio thrust sheets. Moreover, any change in the mechanical properties of the system during its tectonic evolution should be directly reflected in the finite geometry and structural inventory.

The experimental apparatus used is a squeezebox 100 cm in length and 30 cm in width where shortening is achieved by pushing a piston from one side of the otherwise confined box. The experiments feature a layered upper crust with frictional plastic rheology, including strain hardening and softening similar to natural rocks undergoing brittle deformation (Lohrmann et al. 2003). In particular, the model upper crust consists of 5 cm of sieved sand (grain size <630 μm, friction coefficient $\mu \sim 0.6–0.7$; cohesion C ~ 10–100 Pa; density $\rho \sim 1.7$ kg/m^3) overlain by 0.5 cm of glass beads (grain size 70–110 μm, friction coefficient $\mu \sim 0.3–0.4$; cohesion C ~ 10–100 Pa; density $\rho \sim 1.6$ kg/m^3) and 2 cm of sand on top. Sand is a widely used analogue material for a wide range of sedimentary rocks with "normal" shear strength (i.e., a frictional coefficient of about 0.6) (e.g., Lohrmann et al. 2003 and references therein), whereas the glass bead layer represents a low friction detachment corresponding to the Alum shale detachment in the study area. The relatively large thickness of the glass bead layer with respect to nature is an experimental requirement to support strain localization within the weak horizon. Since the alum shale detachment is excavated in the Lockne crater, we model the crater as a frictional heterogeneity by replacing glass beads with sand within a half-circle 10 cm in diameter. To keep the model as simple as possible, morphological crater heterogeneities such as an elevated crater brim or a central crater depression were not considered. To be comparable to natural settings, the experiments must be scaled to nature with respect to length units, density, and cohesion (Schellart 2000). Scaling is expressed in the relationship:

$$(C/\rho g)_{nature}/(C/\rho g)_{exp} \sim K, \quad (1)$$

where C is cohesion, ρ is density, g is Earth's gravity, and K is the scaling factor. Inserting cohesion and density values of the analogue and natural materials at constant gravity, the

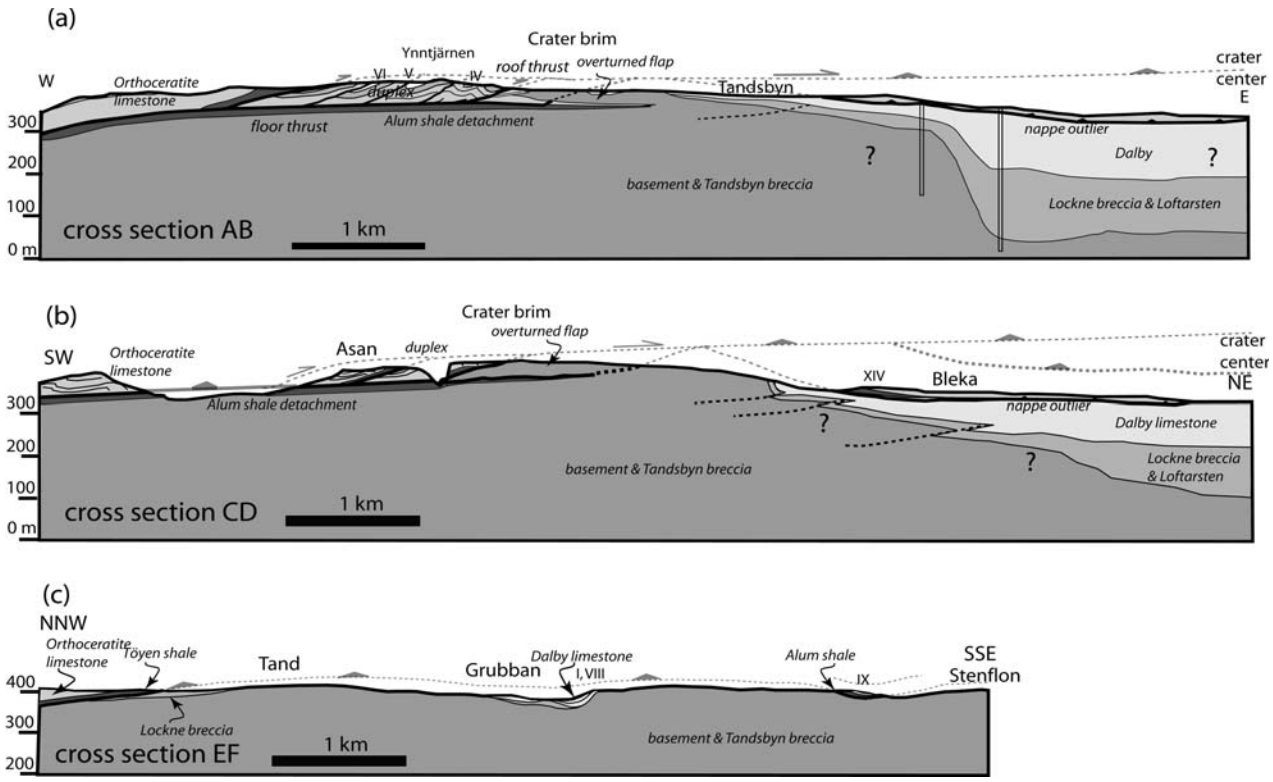

Fig. 6. Geological cross sections of the western part of the Lockne crater and adjacent area. Profiles AB and CD run radially with respect to the crater center, EF is tangentially oriented. The traces of the sections are given in Fig. 5. Cross sections AB and CD show that Caledonian thrusts are stacked west of the crystalline crater brim (ejecta flap) and form a duplex. Section EF displays the gentle syncline that causes the low of the crystalline relief in the Tandsbyn area.

applied scaling factor K is ~10^5, which means that 1 km in nature corresponds to 1 cm in the model. Hence, we simulate shortening of a crust of initially ~8 km in thickness, 30 km in width, and 100 km in length, including a circular crater of 10 km in diameter. Because of the bilateral symmetry of the problem, we simulated a half-space only (i.e., the southwestern half of the crater and adjacent areas), allowing us to analyze the deformation both within and outside of the crater area. Colored sand has been used as marker material to allow monitoring of deformation with a digital camera at constant time steps from beneath, above, and from the side. For further details of sandbox experiments, granular analogue material properties, and scaling principles, see Lohrmann et al. (2003).

From a series of models conducted with the purpose to simulate the deformation and strain partioning at and around the crater heterogenity, we present two experiments: In Model A (3D_18–06), which intended to simulate the deformation in the hanging wall above the detachment, the model upper crust includes an impact-induced, semi-circular frictional heterogeneity. It has been subjected to 29% of shortening at a constant rate of 1.5 cm/min. In Model B (3D_18–09), which intended to simulate the foot wall deformation beneath the detachment, we modified the setup by introducing (i) a 20° inclined detachment ramp geometry and (ii) a thin (0.5 cm) basal film of a Newtonian viscous fluid (silicone putty: viscosity $\eta = 3 \cdot 10^4$ Pas under laboratory conditions: T = 21 °C, shear rate ~10^{-1} s^{-1}). The detachment ramp geometry has been introduced to account for the dipping of alum shale underneath the overriding plate, whereas the viscous base allows a more realistic floating of the brittle upper crust above a ductile lower crust and partitioning of deformation in the foot wall of the shallow detachment. Model B accumulated 48% of crustal shortening at a rate of 1.5 cm/min.

RESULTS

Geological Mapping Campaign

Our geological mapping campaign of the western part of the Lockne crater (Figs. 3 and 4) substantiates previously published geological maps (Lindström et al. 1996; Sturkell 1998a; Lindström et al. 2005a) in many respects, although a number of discrepancies and local deviations occur. It provides new structural data, e.g., of strata orientation (Fig. 4). The exposure of rocks in the Lockne region is fairly good, but in some areas glacial till or soil cover makes geological mapping virtually impossible. Figure 5 displays the outcrop situation. As a precautionary note, we would like to emphasize that only

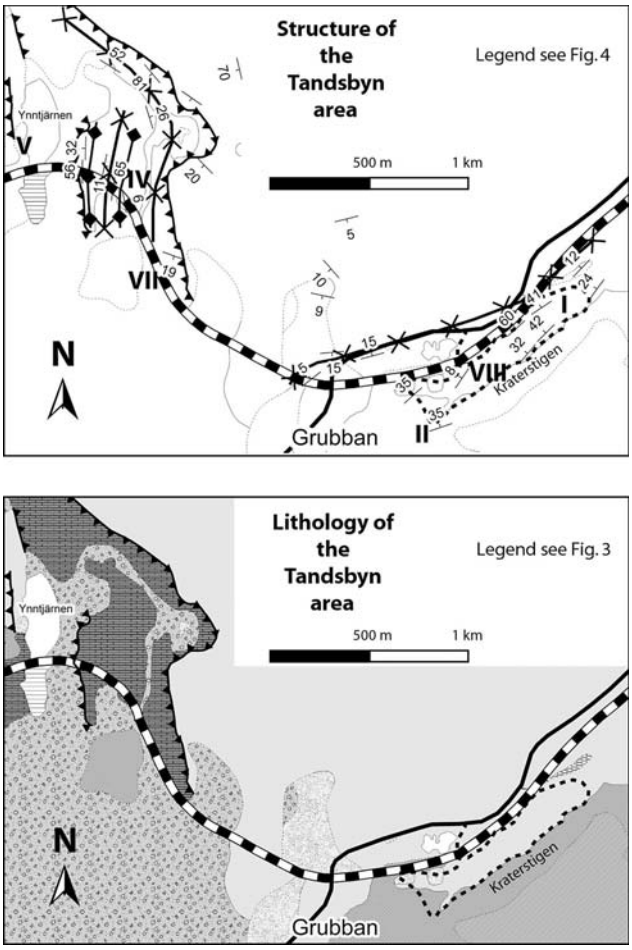

Fig. 7. Close-up of the Tandsbyn area displaying the structure and lithology of the region.

10–15% of the mapped area can be regarded as definitely assured. Hence, all interpretations and models that rely on geological maps of the Lockne area may also bear an uncertainty. We used the same lithological units as reported in Sturkell (1998a); for a petrographical description, we refer to this paper and to Lindström et al. (1996). The lithologies can be grouped into (i) pre-impact, (ii) impact, and (iii) post-impact rocks.

Pre-impact target rocks comprise the Proterozoic crystalline basement, which is mainly built up by Revsund granite, Svekofennian gneisses, metavolcanics, as well as younger sills of Åsby dolerite (Lindström et al. 1996). The pre-impact sedimentary succession amounts to ~81 m of sediments (Sturkell 1998a) and rests on the sub-Cambrian peneplain. Its base is formed by the 28 m thick black, bituminous alum shale of Cambrian age, overlain by an Ordovician succession. Near the base of the Ordovician sequence Töyen shale (Lower Arenigian) occurs overlain by a sequence that is collectively mapped as Orthoceratite limestone (Lower Arenigian to Llandelian). This is a light gray to reddish colored, thickly bedded, and tectonically competent rock with discontinuity surfaces and marly interbeds.

Three types of impactites are distinguished at Lockne, namely Tandsbyn breccia (Lindström and Sturkell 1992), Lockne breccia (Lindström et al. 1983), and Loftarstone (Simon 1987). Tandsbyn breccia is a monomictic crystalline breccia of the inner crater and the brim zone (overturned flap). Transitions to shattered and fractured basement are often gradational. The first deposit that filled the crater cavity as a resurge sediment, which reached a thickness of at least 155 m in the central part of the crater (Sturkell 1998a) (Fig. 6), is named Lockne breccia, a polymictic lithic breccia predominantly composed of partly rounded sedimentary components and few crystalline fragments. It is a clast-supported breccia with clast sizes ranging from a few millimeters to decameter. If single limestone blocks within the Lockne breccia have outcrop-scale sizes, a distinction from Orthoceratite limestone becomes difficult. With increasing distance from the impact center the breccia was deposited at progressively higher stratigraphic levels (Sturkell 1998a) because of the impact-induced erosion. Lockne breccia displays multiple fining upward sequences (Ormö et al. 2007, this issue) and ultimately passes into Loftarstone, a graywacke-like, polymict, arenitic resurge sediment that achieves a thickness of at least 45 m in the central crater (Sturkell 1998a), but only a few meters outside the crater. Both Lockne breccia and Loftarstone occur in the Lower Allochthon nappes west of the crater (Figs. 3 and 6). We did not separately discriminate the monomictic Ynntjärnen breccia (Lindström et al. 2005a) due to gradational transitions to both nodular Orthoceratite limestone and Lockne breccia. We are aware that the Lockne breccia gets more and more monomictic in composition at its base. As long as few crystalline fragments or other lithologies are visible within the breccia and a translation between fragments can be demonstrated we mapped the lithologies as Lockne breccia. If the rock is purely monomictic and a fitting pattern between nodules is present, then we ascribed the lithology as Orthoceratite limestone. The disaggregated nodular limestone near the impact surface may have been formed by weak spallation and subsequent ejecta and resurge dragging (Kenkmann and Ivanov 2006).

The resurge deposits of Lockne breccia and Loftarstone are overlain by marine deposits, suggesting that the marine environment continued directly after the impact (Lindström et al. 1996). The post-impact Dalby limestone (Caradoc) deposited within the crater displays an unusually great lithological variability, both laterally and vertically (Frisk and Ormö, this issue).

Primary Oblique Deposition or Later Tilting?

Strike and dip of bedding planes were systematically measured throughout the crater and are displayed in Figs. 4, 6, and 7. Dip data of post-impact sediments (Dalby limestone)

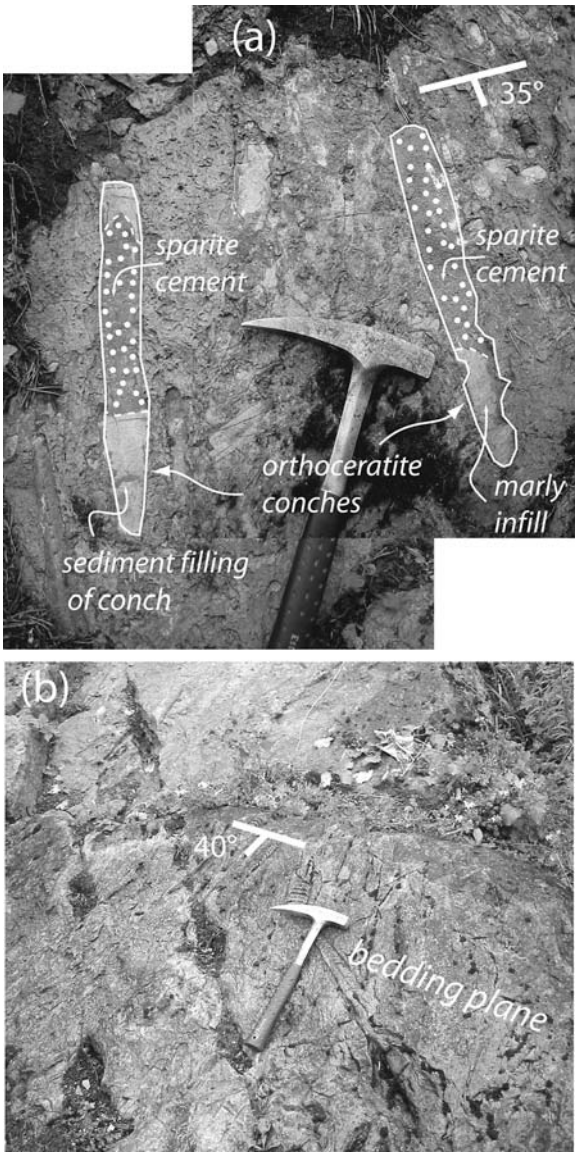

Fig. 8. a) and b) Dalby limestone with Orthoceratite conches at the Kraterstigen circuit (Loc. I, Fig. 7) west of Tandsbyn. The exposed bedding planes continuously dip with 30–40° northwest and contain several Orthoceratite conches that lie within the bedding plane. Conches are partly filled with marly sediment (light gray). Open cavities of the conches were later filled with coarse-grained sparitic calcite cement (stippled). The plane given by the transition from the sparite to the marly infill defines a sub-horizontal plane at the time of deposition (geopetal marker plane). Photographs document that this plane is parallel to the bedding plane indicating a sub-horizontal deposition of bedding planes.

give the tilting of strata and can be attributed to a tectonic overprint onto the crater if the bedding planes were deposited horizontally. We used geopetal markers as well as the preferred alignment of internal sedimentary fabrics to prove this assumption.

Orthoceratite conches (Fig. 8) are often useful geopetal markers and are therefore critical in assessing the primary

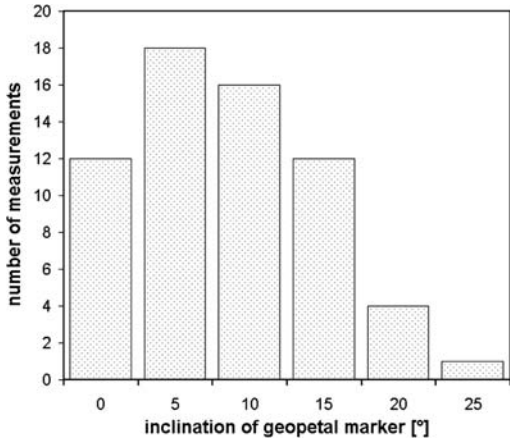

Fig. 9. Histogram shows the angle measurements between geopetal marker plane and bedding plane.

inclination of bedding planes at the time of deposition. Orthoceratites are very frequent in outcrops of the post-impact Dalby limestone in the Tandsbyn area (e.g., Loc. I; Fig. 7). Their long axes are always oriented parallel to bedding. Occasionally, conches are aligned parallel to each other on bedding planes suggesting deposition in a current (Fig. 8a). Partial filling of the chambered conches with marly sediment gives information on the orientation of a horizontal. plane at the time of deposition. Analyzing numerous conches (Fig. 9) we found that the angle between the geopetal marker plane and the bedding plane ranges between 0–25° with an average of 5°–10°. One must take into consideration that the geopetal markers itself may have an error of ~10°. Local deviations from a horizontal plane occur because the conch chambers get filled through a tube that connects the chambers. Intruding sediment sometimes forms a small sediment fan with an apex near the tube. In such cases the marker plane often has a concave shape.

The internal fabric of sediments gives further clues to the deposition angle. If the bedding plane of a bed is oriented parallel to elongated shells, detritus, and clasts of that bed the deposition most likely occurred horizontally. In opposite, if elongated and aligned particles of a bed form an angle to the bedding plane of that bed the deposition occurred at a slope. Our statistical fabric analysis (Fig. 10a) reveals that shells and elongated particles are aligned sub parallel to the bedding plane making a deposition at a slope unlikely. Since the bedding plane of Fig. 10a (Loc. II; Fig. 7) dips with 35° northwest a later tectonically induced rotation in a fully lithified state is indicated.

The two independent methods indicate that the bedding planes of the post-impact Dalby limestone were formed sub-horizontally or at gentle slopes not steeper than 5–10°. The present inclination of these bedding planes is thus the sum of primary bedding inclination (0–10°) and later rotation in a lithified state, most likely during Caledonian

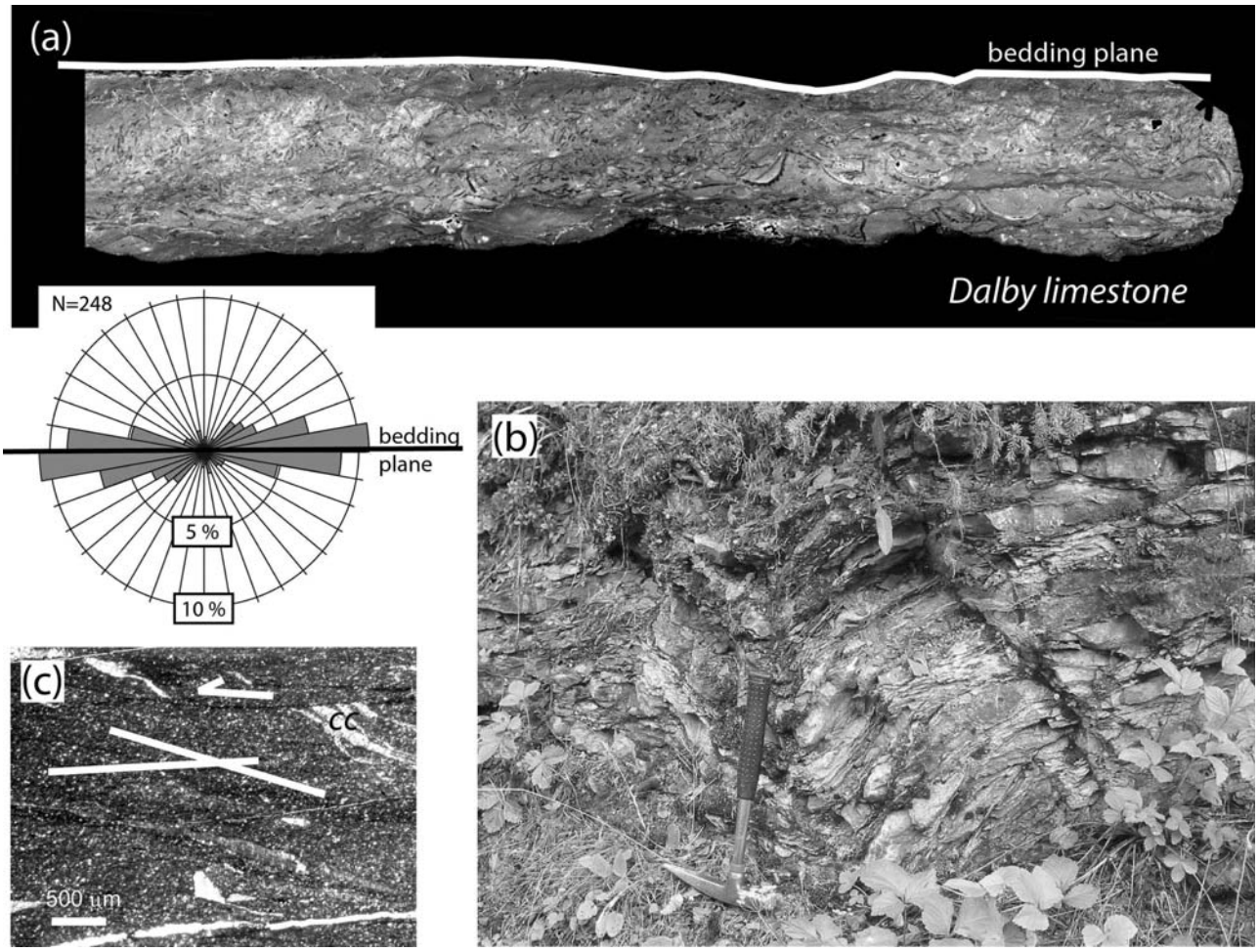

Fig. 10. a) Orientation analysis (rose diagram) of shells and elongated particles of Dalby limestone shows a shape-preferred orientation parallel to the bedding plane and suggests a primarily sub-horizontal deposition. The sample is from the Kraterstigen trail at the southern Tandsbyn syncline limb (Loc. II; Fig. 7). Inclination of bedding is 35°. b) Meter-scale fold in Dalby limestone (Loc XIII; Fig. 7). The fold is exposed near the entrance of the Kraterstigen circuit. c) Microstructural analysis of slates of (b) revealed that folding resulted from tectonic deformation of solid rock, not from slumping in an unlithified state. Note the acute angle between bedding and slaty cleavage, localized shearing and strained calcite-bearing tension gashes (c).

thrusting. A contribution of differential compaction on tilting of the sediments can be ignored because the sedimentary sequences are too thin near the contact to the crystalline basement to account for this effect. Dip values in the Kraterstigen area (Loc. I, II, VIII; Figs. 6c and 7) which represents the southern part of the proposed "Tandsbyn gully" (Fig. 2) are usually 30–40° and occasionally up to 60°. Such values indicate a strong tectonical rotation. We therefore rule out that the Tandsbyn area was a primary low in the crater brim as suggested by Lindström et al. (1996) and von Dalwigk and Ormö (2001). We suggest it became a low due to later deformation. Our results are in contrast to previous and recent work by Lindström, Ormö, and co-workers (e.g., von Dalwigk and Ormö, 2001; Ormö et al., this issue; Frisk and Ormö, this issue) who interpreted inclined bedding planes as primary depositional features that were not affected by later tectonic rotation.

Post-Impact Caledonian Deformation

Since the Dalby limestone was deposited after the impact, it can record the post-impact deformation history only. Deformation affected these rocks must have also affected the crater itself if no detachment exists between Dalby limestone and the underlying impactites. About 6 km west of the crater center, still within the shallow outer crater, Dalby limestone, Lockne breccia, Loftarstone, Orthoceratite limestone, and Tandsbyn breccia are incorporated into the frontal Caledonian nappes (e.g., Loc. IV; Figs. 3–5, 6a, 7, and 11). Folds in these rocks are formed as detachment folds (Loc. IV; Figs. 5, 6, and 11a), fault-bend folds, and fault-propagation folds (Loc. V; Figs. 7, 11b). For thrust terminology we refer to McClay (1992). Figure 11b shows the vertical limb of an anticline that generated above a thrust ramp tip. Several ramps branch into a basal detachment plane

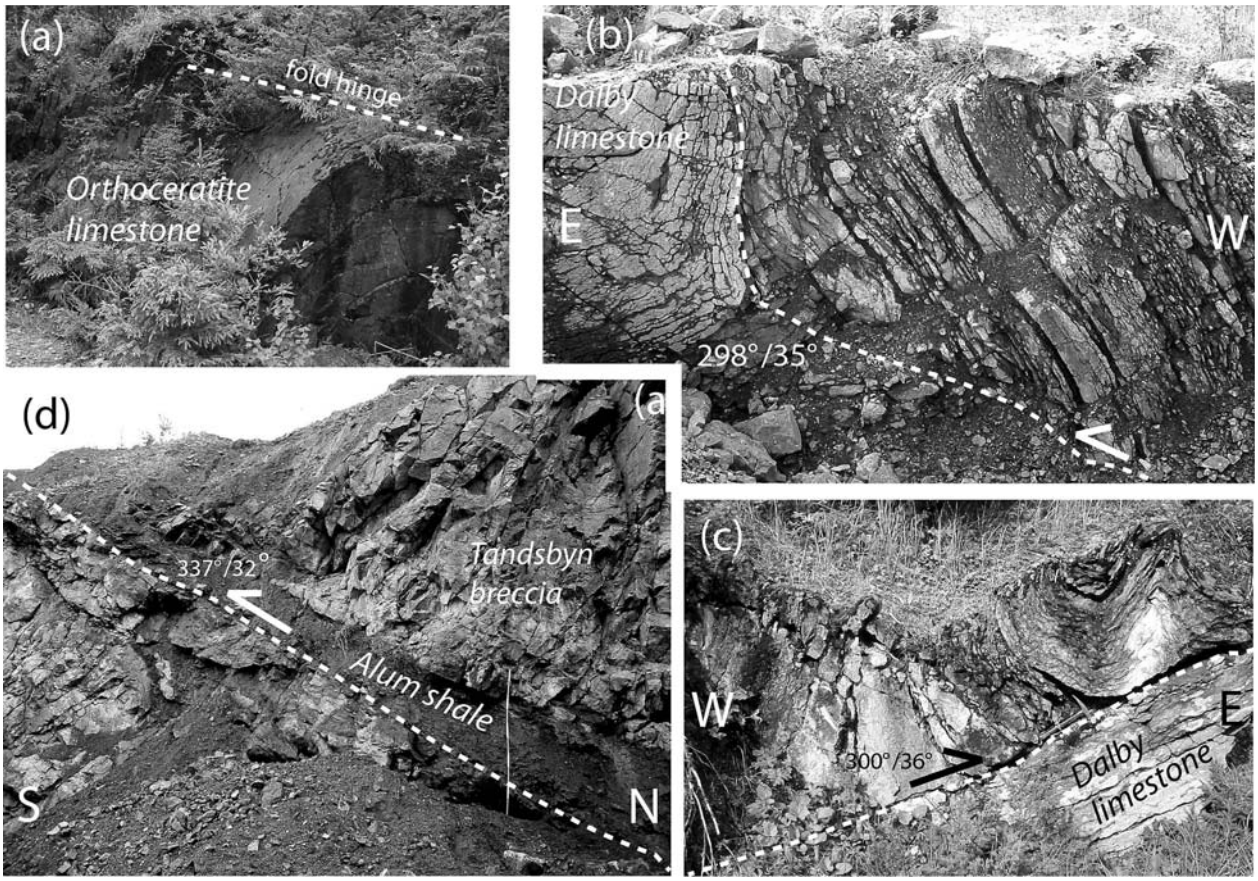

Fig. 11. Photographs of various outcrops west of the crater in the Tandsbyn area (a–c) and at Nordanbergsberget (d). a) Folding of Orthoceratite limestone above the detachment (Loc. IV). b) East-vergent fault-propagation fold above a tip of a thrust ramp west of Lake Ynntärnen. The outcrop shows the overturned eastern limb of the anticline (Loc. V). c) Asymmetrical meter-scale chevron-style folds above a bedding-parallel ramp within Dalby limestone (Loc. VI; Railway section). d) Tectonically induced ramp in alum shale at Skanska quarry, Nordanbergsberget (Loc. XIII).

(Figs. 6a and 6b). The Cambrian alum shale is the major detachment horizon outside the inner crater (Fig. 6). Along an east-west section in the western part of the outer crater (Loc. IV and VI; Figs. 5, 6, 11) the above mentioned lithologies display multiple repetitions and folds with overturned eastern fold limbs that indicate the movement direction of thrust slices. Folding is accommodated by flexural slip (Figs. 11a–c) and concentrates on marly interbeds of the Orthoceratite limestone and Dalby limestone.

Further east (Loc. VII, Figs. 5 and 7) and beneath the alum shale detachment, the intensity of folding and faulting decreases. Folds become open, and the spacing between faults gets larger. In the Tandsbyn area (Fig. 7) (named "Tandsbyn gully" by Lindström et al. 1996; von Dalwigk and Ormö 2001; Fig. 2) Dalby limestone dips with 30–40° northwest (Fig. 7); locally a tilt of 60° northwest is measured at Kraterstigen. This area is interpreted as the southeastern limb of an east-northeast trending open syncline (Fig. 6c). The northwestern limb of this synform dips more gently and is poorly exposed. Small-scale subsidiary folds trend parallel to the syncline axis (Loc. VIII; Figs. 7, 10b, and 10c). Folding of Dalby limestone (Fig. 10b) occurred in a lithified state that led to their formation of slaty cleavage and tension gashes filled with calcite (Fig. 10c). The latter were sheared and strained after their formation (Fig. 10c). We therefore suggest that this meso-scale folding is not caused by unlithified slumping at a slope, as proposed by Lindström (personal communication).

At Långmyren (Loc. IX; Figs. 5 and 6c), 4 km south-southwest from the crater center, we found deformed limestone presumably of Early Ordovician age (Orthoceratite limestone, Ceratopyge limestone) underlain by alum shale (Figs. 3, 4). This sequence, it is interpreted as a relic of a nappe overthrusting the crater brim (Fig. 6c).

About 4 km south of the crater center (Loc. X; Fig. 5, Bergböle area, named "Bergböle gully" by Lindström et al. 1996 and von Dalwigk and Ormö 2001, Fig. 2) Dalby limestone, Loftarstone, and Lockne breccia are exposed. All lithological units show inclined bedding planes from which a northwest-southeast–trending monocline and subdued syncline (Fig. 4) with an axis plunging towards the crater

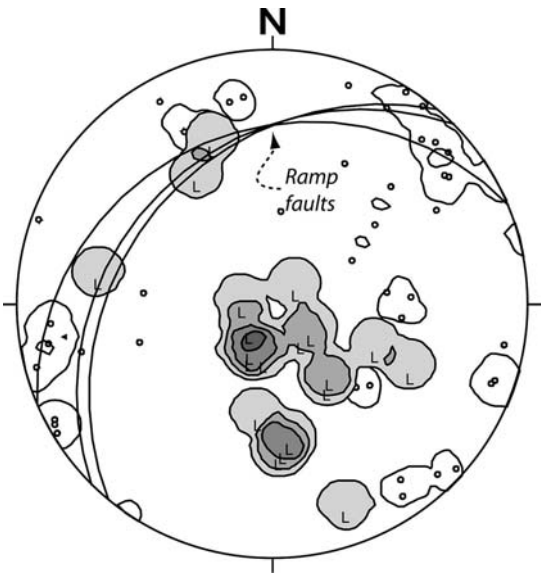

Fig. 12. Stereographic projection (Schmidt projection, lower hemisphere) of fault-slip data measured at Nordanbergsberget (Loc. XIII). Displayed are poles of fault planes (circles; N = 46) and lineations on these faults (L; N = 20).Density contours of fault plane poles are unshaded (4.4, 8.8%), density contours of linears are gray-shaded (5, 10, 15, 20%). North-south–trending lineations on steep normal faults can be correlated to the impact of the overturned flap on the surface. northwest-dipping slip vectors on northwest dipping reverse faults (great circles) are correlated with Caledonian thrusting (see Fig. 11d).

center can be constructed. Dip angles of strata are in the order of 15–20°. West of this area the top of the Precambrian crystalline bedrock is exposed at 435 m (Loc. XI; Fig. 5), 1 km farther east at 340 m (Loc. XII; Fig. 5). The eastern part of this structure is not exposed. In analogy to modeling, we interpreted this area as being affected by a basement ramp fault that causes the large throws of the basement (see next section).

Our field studies suggest that the Baltoscandian foreland and with it the impact crater itself was indeed affected by the Caledonian orogeny in the Lockne area (Fig 6). However, the strikes of strata and the trend of fold axes in the foreland deviate remarkably from the standard Caledonian directions (northeast-southwest) showing radial and concentrical orientations with respect to the proposed impact center at the western shore of Lake Locknesjön.

We analyzed fault kinematics at the quarry of Nordanbergsberget (Loc XIII; Fig. 5, 4 km north of the crater center), the prime locality where the overturned crystalline ejecta flap is resting on a thin veneer of alum shale. Fault-slip analysis (Fig. 12) revealed a two-fold trajectory pattern: i) One set shows preferred north-south–trending lineation on steeply dipping normal faults. This set can be correlated with the ejection process and emplacement of the flap. The normal faults may have been activated when the overturned flap hit the surface: the crater near parts of the overturned flap impact the surface earlier than the distal parts and cause displacements within a coherent ejecta flap. In other words, an inner part of the flap has already encountered the surface and come to rest while the outer continuation is still in flight. ii) A second set of faults display northeast strikes and northwest-southeast slip vectors that indicate a Caledonian overprint (Figs. 11d and 12). As the elevated brim zone represented an obstacle for nappe propagation, southeast shearing of the overturned brim on the alum shale veneer was common. Locally alum shale is squeezed out to higher levels and covers fault planes.

Shallow Thrusting and the Geometry of the Caledonian Alum Shale Detachment

Over large parts of the eastern Caledonian thrust front in Scandinavia the alum shale detachment effectively decoupled the autochthonous Baltoscandic foreland from the deformed Parautochthon to basal Lower Allochthon nappes. In the vicinity of the Lockne crater, erosion has exposed parts of the sub-Cambrian peneplain and overlying alum shale (Sturkell and Lindström 2004). A regional drilling program made it possible to reconstruct the westward continuation of the peneplain beneath the cover of the Caledonian thrusts (Andersson et al. 1985). Due to flexural loading by the orogenical belt the sub-Cambrian peneplain dips evenly with 0.7~0.85° toward the northwest (Andersson et al. 1985; Sturkell and Lindström 2004). In the area surrounding the Lockne crater, however, the surface and elevation level of the sub-Cambrian peneplain and alum shale substantially deviate from what can be expected from its general trend. Sturkell and Lindström (2004) calculated deviations from a mathematically defined peneplain and found, e.g., a negative deviation of –119 m southeast of the crater at the shoreline of Lake Locknesjön. This was interpreted as down faulting along steep northwest-striking faults (Sturkell and Lindström 2004; Lindström et al. 2005a) which may or may not be related to the Caledonian orogeny. Based on the same data (Andersson et al. 1985; Sturkell and Lindström 2004; Lindström et al. 2005a), we compiled the sub-Cambrian peneplain and hence the alum shale detachment surface, making use of the kriging grid interpolation method. As can be seen in Fig. 13, perturbation of the otherwise smoothly dipping plane occurs in the surrounding of the Lockne crater. The detachment is deflected to a lower level northwest of the crater. The northeastern and southern crater is flanked by local highs. Southeast of the crater the detachment occurs at an unusually low level. The perturbation of the surface around the impact crater displays some bilateral symmetry. The symmetry axis (northwest-southeast) coincides with the principal axis of shortening in the Caledonides (Fig. 13). The systematic change in surface morphology including its bilateral symmetry around the crater suggests a causal relationship.

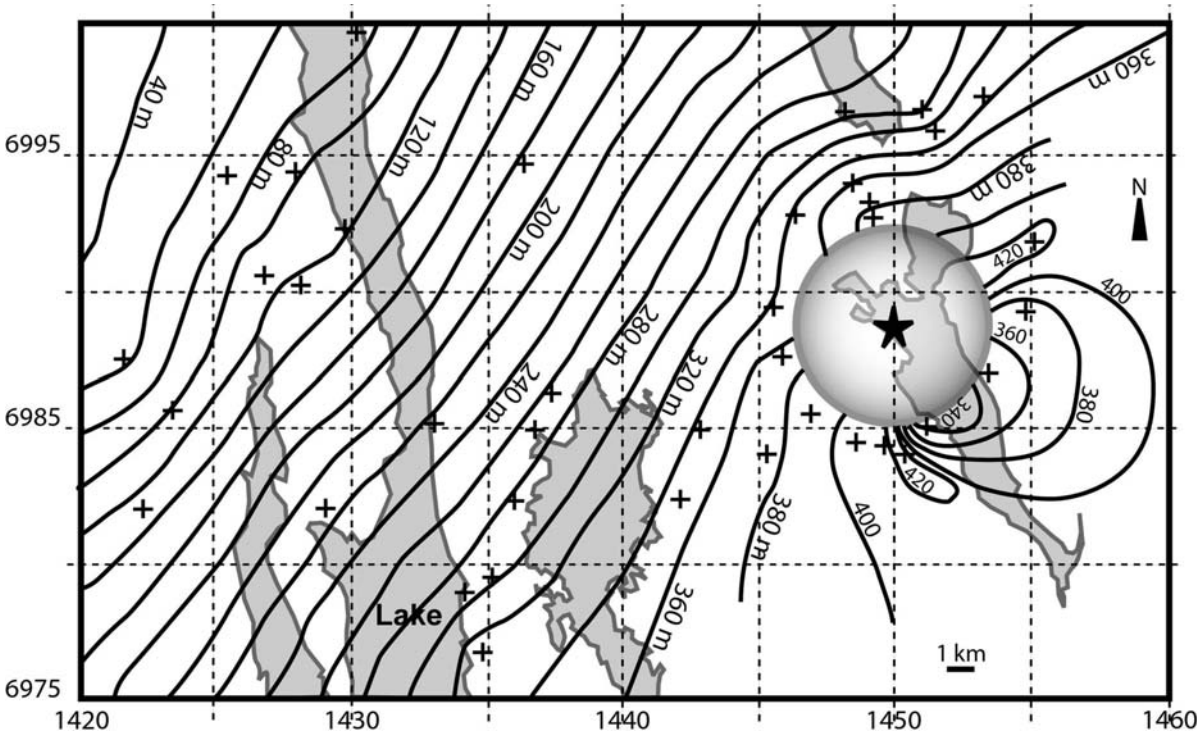

Fig. 13. Topography of the sub-Cambrian peneplain and overlying alum shale in the surrounding of the Lockne area based on data provided by Andersson et al.(1985), Sturkell and Lindström (2004), and Lindström et al (2005a). Note the perturbation of the surface in the vicinity of the crater. See text for discussion.

The innermost exposure of alum shale in the crater occurs in the hinge zone of the overturned flap of the ejecta brim at Nordansbergberget (Loc. XIII; Fig. 5) but is also expected at other localities of the brim zone beneath the crystalline ejecta (Figs. 6a and 6b). However, occurrences of alum shale also exist on top of the crystalline ejecta brim, e.g., in the south (Loc. IX; Figs. 5 and 6c). This indicates that alum shale locally got stuck at the base of a thrust sheet and thrusted onto the brim of the crater. Within the inner part of the Lockne crater, the Cambrian alum shale is lacking because it was excavated during the impact that occurred about 30 Ma before the region was involved in orogeny. However, an outlier of the Caledonian nappes is situated within the central crater depression (Figs. 3 and 4). The base of this nappe that was drilled in two boreholes (Lindström et al. 1996) is at about 300 m, hence 100–120 m beneath the average detachment base outside the inner crater along northeast-southwest striking (Fig. 6b). This indicates a sagging of nappes when they approached the crater depression. The exposed detachment of this nappe outlier is Lower Ordovician Töyen shale (Loc. XIV; Fig. 5). Töyen shale is separated from alum shale by a few meter thick limestone sequence. We conducted a strain analysis that revealed dominant shortening in a northeast-southwest and east-west direction which is inconsistent with the standard principal axis of shortening of the frontal Caledonian nappes (northwest-southeast).

Analogue Modeling

Scaled analogue experiments yield a first-order approach to understanding the internal structural evolution and related particle displacement field of fold-and-thrust belts. Here we have focused on the effect of a circular high-friction heterogeneity representing the Lockne crater embedded in a low-friction detachment plane (alum shale detachment) on thrust propagation during wedge formation in a compressive regime (the Caledonian orogenesis). More specifically, we studied the deformation field around the crater area in the hanging wall (Model A) and in the foot wall (Model B) in order to infer the pattern and mechanisms of strain partitioning associated with this mechanical heterogeneity.

Crustal shortening during the experiments is consistently accommodated in two steps: i) Thick-skinned basement thrusting during early stages of the evolution, followed by ii) activation of the shallow detachment (alum shale detachment) and the change to thin-skinned folding and thrusting. In the context of the critical taper theory, early thick-skinned basement thrusting allows the wedge to reach its critical taper controlled by cohesion and internal and basal friction. Once the geometry of the dominantly upward growing wedge has adjusted to the controlling parameters (i.e., is critical), the deformation front propagates outward resulting in self-similar growth of the wedge. In the presence of a shallow detachment,

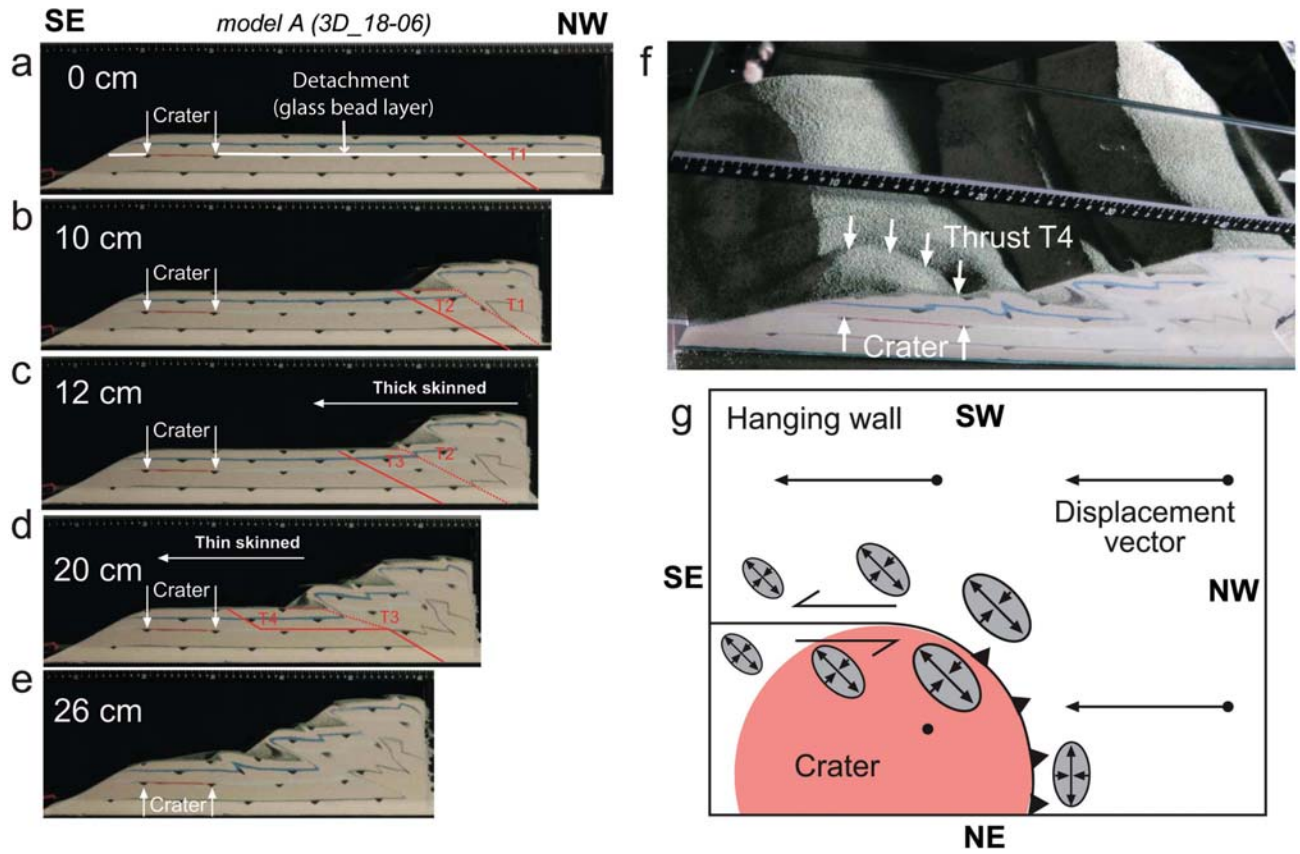

Fig. 14. Structural evolution of Model A (3D_18–06): The model simulates a brittle upper crust (sand layers) with a shallow detachment (thin glass beads layer) in which a frictional heterogeneity occurs (crater). a) Thrusting starts with the activation of a basement thrust 1 (T1). b) Initiation of a second basement thrust 2 (T2) and simultaneous deactivation of T1 after 10 cm of convergence. c) A third basement thrust (T3) forms after 12 cm of convergence and accommodates about 8 cm of convergence until (d) the glass bead horizon is activated as a shallow detachment (T4). e) Final stage of experiment after 26 cm of shortening. f) Oblique top view of the sand box after 26 cm of shortening. g) Inferred qualitative kinematic model and strain partitioning (indicated by ellipses) in the hanging wall of the detachment horizon.

which changes the frictional parameters at the base of the growing wedge, the wedge has to adjust accordingly by decreasing its taper. This adjustment is reached by the onset of thin-skinned folding and thrusting. The presence of any frictional heterogeneity within the shallow detachment will result in a renewed adjustment of the wedge by fault activation or changes in tectonic style as will be shown below.

Model A (3D_18–06) (Fig. 14): Shortening of a Brittle Crust Including a Horizontal Detachment

Shortening started with the activation of a basement thrust 1 (T1) near the piston (Fig. 14a). After 10 cm of convergence (11% of shortening), initiation of a second basement thrust 2 (T2) and simultaneous deactivation of T1 occurs when a critical slope angle is reached (Fig. 14b). A third basement thrust (T3) forms after 12 cm of convergence (13% of shortening) and accommodates about 8 cm of convergence until the glass bead horizon is activated after 22% of shortening as a shallow detachment (simulating the alum shale detachment). This change from thick-skinned to thin-skinned tectonics causes “fast” propagation of deformation into the foreland (Fig. 14c). Sliding on the detachment, however, is aggravated where the crater heterogeneity is located (front side of the model) resulting in the localization of shortening at the crater brim represented by the formation of thrust T4 (Fig. 14d). The oblique top view of the sand box (Fig. 14f) after 26 cm of convergence (29% of shortening) shows that the ramp fault T4 follows the curvature of the high-friction heterogeneity. It extends as a lateral ramp and is connected with the active shallow detachment that has approached the eastern end of the model box. This lateral ramp is a zone of left-lateral shearing between the nappe (outside of the crater area) and the locked part above the crater heterogeneity. A qualitative kinematical model inferred from this structural evolution and the associated strain field within the hanging wall of the detachment horizon is shown in Fig. 14g. Due to left-lateral shear the principal axis of shortening in the vicinity of the crater is oriented at 45° to the strike of the lateral ramp. In contrast, the orientation of the principal axis of shortening in the far field outside the heterogeneity is perpendicular to the deformation front. The strain tensor south of the crater has

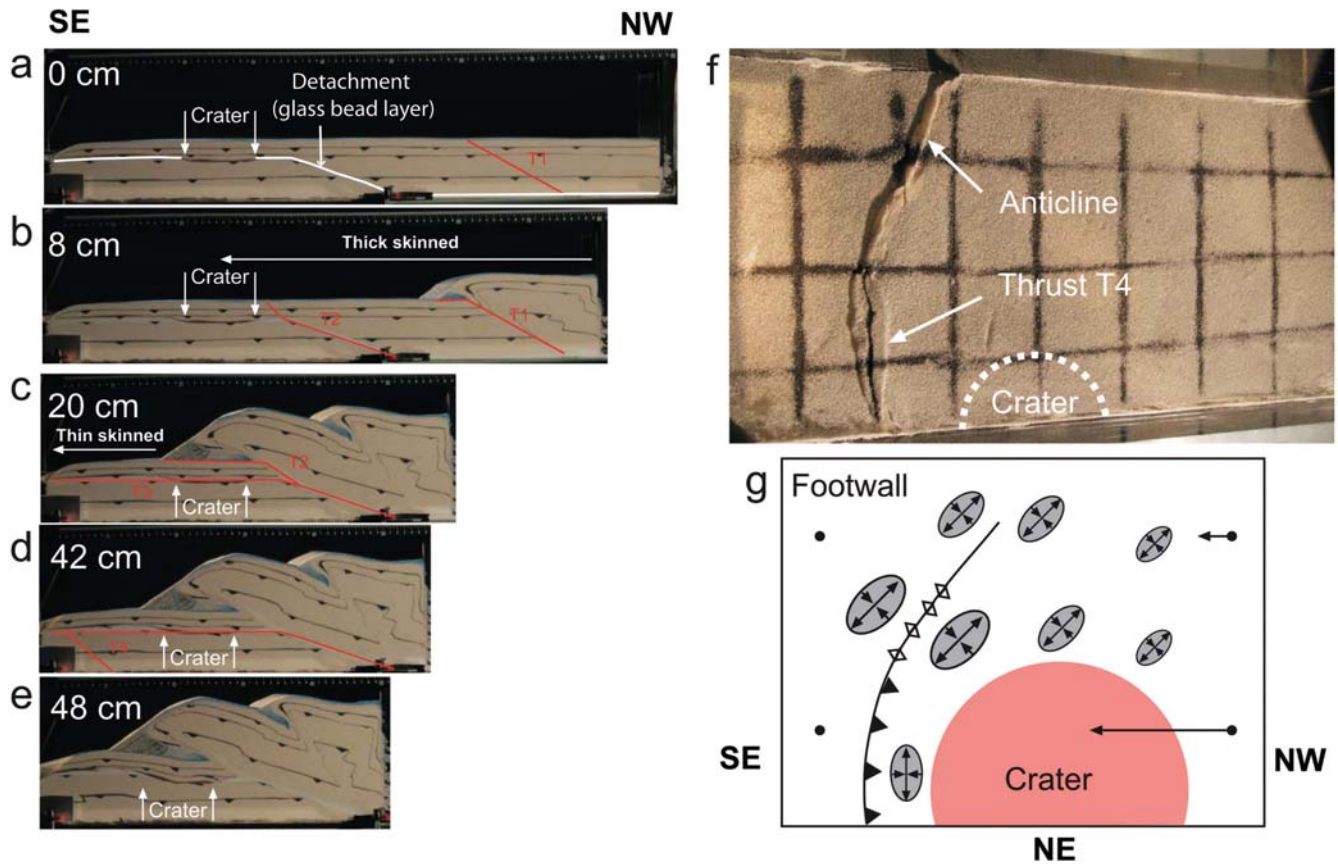

Fig. 15. Structural evolution of Model B (3D_18–09). The model simulates a brittle upper crust (sand layers) above a ductile middle-to-lower crust (silicone putty). The shallow detachment (thin glass beads layer) has a northwest-dipping part and a flat part in which a frictional heterogeneity occurs (crater). a) Thrusting starts with the activation of a basement thrust 1 (T1). b) Initiation of a second basement thrust 2 (T2) and simultaneous deactivation of T1 after 8 cm of convergence. c) Activation of the glass bead horizon (T3) and partial deactivationof T2 after 20 cm of convergence. d) Activation of T4 after 42 cm of convergence. e) Final stage of experiment after 48 cm of convergence. f) Oblique top view of the silicone layer after 48 cm of convergence. (g) Inferred qualitative kinematic model and strain partitioning (indicated by ellipses) in the foot wall of the detachment horizon.

consequently rotated anticlockwise by about 45° in response to the heterogeneity (Fig. 14g).

Model B (3D_18–09) (Fig.15): Shortening of a Brittle Crust Including an Inclined Detachment Above a Ductile Substratum

The principle evolution of the wedge in Model B is similar to Model A with a change from thick-skinned basement thrusting to thin-skinned folding and thrusting after 22% of shortening (Figs. 15a–c). However, the detailed evolution of the wedge differs due to the modifications of model parameters. First, the ramp geometry of the glass beads detachment reduced friction at the base of the thick-skinned wedge and caused the formation of two thrusts (T1 and T2) instead of three enclosing thrust sheets with higher aspect ratios. Second, the presence of a silicone putty film on the floor of the box (mid-crustal ductile layer) allowed shortening to be accommodated along a basal plane and hence deformation to be partitioned into the "floating" crustal block beneath the crater area, i.e., the foot wall with respect to the detachment horizon, that has not been subjected to deformation in Model A. Like in Model A, the high-friction heterogeneity area of the crater hinders movement along the shallow detachment. Instead of accommodating shortening in the crater area within the nappe itself (i.e., the hanging wall) as has been observed in Model A, in Model B, shortening is accommodated in the foot wall first by diffuse deformation below the shallow detachment in the crater area and later by decoupling of the upper crust from the ductile substratum. After 42 cm of convergence (47% of shortening), deformation below the crater area is localized along a basement thrust T4 (Figs. 15d and 15e), indicating a change from thin-skinned deformation back to thick-skinned deformation in the crater area.

Removal of the deformed sand layers at the end of the experiment revealed (Fig. 15f) that thrust T4 passes laterally (southwestward) over into a curved anticline. Figure 15g shows a qualitative kinematical model inferred from the observed structural evolution and the associated strain field within the foot wall of the detachment horizon. Accordingly, a lateral gradient in shortening may cause a right-lateral shear

component at the southern side of the heterogeneity. This is consistent with an up to 45° clockwise rotation of the strain tensor in the vicinity of the crater with respect to the regional orientation (long axis parallel to deformation front).

To summarize both experiments, we can adhere to the following: accommodation of convergence-induced shortening by thrusting above a shallow detachment is hindered where the high-friction crater heterogeneity is situated, causing strain partitioning, internal deformation both in the hanging wall and foot wall, and non-plane strain deformation. Hanging wall (nappe internal) deformation may include the initiation of a circumferentially striking ramp fault at the crater brim delineating the high-friction heterogeneity at the nappe base (Model A) (Figs. 14f and 14g). Crustal shortening in the crater area may also be accommodated locally by the activation of a mid-crustal detachment or lower crustal flow, resulting in the activation of basement thrusts and diffuse shortening in the foot wall crater area, which decreases laterally outward (Model B) (Figs. 15e–g). Strain gradients both vertically and horizontally result in non-plane strain deformation in the vicinity of the crater characterized by a deviation of the local finite strain tensor orientation with respect to the regional orientation (long axis parallel to the deformation front) by up to 45° and by up to 90° to each other in the hanging and foot walls. In particular, strain tensors to the south of the crater center may rotate clockwise in the foot wall and anticlockwise in the hanging wall of the shallow detachment and in opposing senses to the north of the crater center.

DISCUSSION AND CONCLUSION

Correlation of Nature and Modeling

The formation of the Lockne crater 455 Ma ago created a particular geological configuration that was unique in the Baltoscandian foreland and caused specific adjustments when the fold and thrust belt of the Caledonides reached and overthrusted the crater ~30 Ma later. Special characteristics of the Lockne area at the Scandian period of the Caledonidian orogeny were (i) the presence of a crater depression due to an incomplete filling of the crater with post-impact sediments, (ii) an elevated brim zone of ejected crystalline rocks surrounding this depression, and (iii) the lack of alum shale and *Töyen shale* that could be used as an appropriate detachment plane throughout the eastern Caledonian thrust front. While the effect of (iii) on the deformation behavior in a fold-and-thrust belt was analyzed with the help of analogue modeling (see above), (i) and (ii) are assessed on the basis of field data and theoretical considerations.

The presence of a depressed inner crater basin that is formed beneath the level of the main alum shale detachment could lead to a sudden downward depression of a propagating thrust sheet. Once it has filled and leveled the depression it may activate an out-of-sequence thrust at its rear to form a roof thrust on top of the first one (Figs. 6a and 6b). Its lateral extent is limited by the dimension of the circular basin. Hence, the frontal thrust ramp would laterally pass into an oblique ramp, a side-wall ramp and/or a tear fault. This scenario is in agreement with the observed nappe outlier situated in the crater depression with a base more than 100 m below the standard nappe base.

The elevated brim of the crater, composed of monomictic crystalline breccia (*Tandsbyn Breccia*), has acted as an obstacle (Lindström et al. 2005a). Southwest of the brim, Lindström et al. (2005a) mapped five northwest-southeast–trending anticlines with wavelengths of 0.5–1 km and amplitudes not over 50 m, indicating a northwest-southeast shortening of not more than 200 m. A similar magnitude of shortening was derived for the northwest sector. In all cases, the antiforms strike tangentially to the crater, indicating that the crystalline brim zone in fact acted as an obstacle. Figures 4, 6a, and 6b show that these folds are associated with ramp faults. The allochthonous rocks west of the crater brim form imbricate thrusts that link a floor thrust at the level of the alum shale to a roof thrust at the level of the crater brim top (Figs. 6a and 6b) and form duplex structures.

Alum shale as the ideal low-friction detachment is lacking in the inner Lockne crater. The effect of a circular high-friction heterogeneity in the glide plane on the overthrusting kinematics was analyzed by analogue experiments. We have documented that nappe internal deformation may include the initiation of a circumferential striking ramp fault at the crater brim delineating the crater (Figs. 6a and 6b). Relics of nappes occur in the crater center, on top of the crater brim, and surrounding the crater brim. Strain analysis in the Töyen shale at the southern edge of the central crater nappe outlier (Loc. XIV; Fig. 5) revealed northeast-southwest shortening consistent with the findings of Model A (Fig. 14g). The tangential trend of fold axes and ramps in the southwest, west, and northwest sectors of the outer crater (Lindstöm et al. 2005a) is also in accordance with the model. The presence of several thrust ramps in the southwest (Fig. 6b), west (Fig. 6a), and northwest sectors of the Lockne crater correlates with ramp formation west of the crater as a result of thrust propagation hold-up.

Although our analogue models are not designed to precisely match nature, they provide useful insights for understanding the deformation behavior of hanging wall nappes and the foot wall crater. Modeling showed that the detachment anomaly changes the strain partitioning between hanging wall thrusts and the foot wall foreland and causes vertical and horizontal strain gradients. Deformation of the foot wall crater area gets important if a deeper detachment is activated, most likely near the brittle-to-ductile transition at mid-crustal levels. The occurrence of a ramp fault at the southeastern margin beneath the modeled crater (Model B; Figs. 15 e–g) finds a striking correlation at the Lockne crater.

The mapped surface of the sub-Cambrian peneplain and associated alum shale detachment (Fig. 13) (Loc. XI and XII; Fig. 5) provides a good marker for foot wall deformation around the crater. Sudden level changes of about 80 m at the southeastern border of the crater strongly suggest the existence of a ramp fault like in the analogue model.

Differences in the amount of lateral shortening cause a rotation of the strain tensor. Applying the results of analogue modeling (Model B); Fig. 15g) to the Lockne crater (Figs. 3, 4) means that the principal axis of shortening in the foot wall to the west of the crater center is about east-west, which is consistent with the trend of the Tandsbyn syncline and related strike of strata in the Tandsbyn area. The orientation of the subdued structure at Bergböle (Loc. X–XII; Fig. 5) seems not to fit to the predictions from the model. However, this region seems to be influenced by the foot wall ramp fault at the southeast margin of the crater. This ramp could be responsible for the vertical offset of the alum shale detachment.

"Resurge Gullies" versus "Deflected Tectonics"

The formation of radially oriented resurge gullies in marine impact craters cutting through a pre-fractured ejecta brim (Fig. 2) with lows and highs is a plausible mechanism during backwash, particularly for shallow water if the back surging water height is similar to the crater brim height. In this case the crater brim could act as a dam. The local bursting of the dam-like brim might form radially oriented gullies. Nevertheless, their importance at Lockne seems to be overestimated: At the "Tandsbyn gully" (Figs. 2 and 7) we found that the post-impact sediments above the resurge deposits (Dalby Limestone) dip toward the gully center by 20–40°, sometimes up to 60° (Loc. I, II; Figs. 6c and 7). Even if a primary oblique deposition of bedding planes at angles of 10° and more is taken into account a considerable subsequent tectonic tilting is necessary. Restoration of this tectonic folding to the original unfolded state may result in the elimination of the radially oriented basement troughs (gullies). We therefore propose that "resurge gullies" at Lockne are the result of a preferred preservation of resurge deposits in gentle synclines that have formed during the Caledonian thrusting event. The orientation of syncline axes more or less radial to the crater is interpreted to be the result of a rotation of the local finite strain tensor due to strain partitioning in the vicinity of the crater.

Acknowledgments–We would like to thank the organizers for a scientifically inspiring and logistically perfect meeting. We are particularly grateful to Maurits Lindström and Jens Ormö for various advices and open-minded discussions in the course of the field campaign and during the workshop. We acknowledge the helpful reviews by E. Turtle and an anonymous reviewer and thorough editing by A. Deutsch. We would like to express our thanks to N. Kukowski and O. Oncken for enabling the use the analogue laboratory at GFZ-Potsdam. We are grateful to B. Kröger (Museum of Natural History Berlin) for his help with the allocation of rocks to the Ordovician stratigraphy. We also acknowledge the preparatory work by H. Knöfler.

Editorial Handling—Dr. Alexander Deutsch

REFERENCES

Andersson A., Dahlman B., Gee D. G., and Snäll S. 1985. The Scandinavian alum shales. *Sveriges Geologiska Undersökning* C56:1–50.

Davis D., Suppe J., and Dahlen F. A. 1983. Mechanics of fold-and–thrust belts and accretionary wedges. *Journal of Geophysical Research* 88:10,125–10,133.

Earth Impact Database. 2007. http://www.unb.ca/passc/ImpactDatabase. Last accessed January 31, 2007.

French B. M., Koeberl C., Gilmour I., Shirey S. B., Dons J. A., and Naterstad J. 1997. The Gardnos impact structure, Norway: Petrology and geochemistry of target rocks and impactites. *Geochimica et Cosmochimica Acta* 61:873–904.

Frisk A. M. and Ormö J. 2007. Facies distribution of post-impact sediments in the Ordovician Lockne and Tvären impact craters: Indications for unique impact-generated environments *Meteoritics & Planetary Science* 42. This issue.

Gee D. G. and Kumpulainen R. 1980. An excursion through the Caledonian mountain chain in central Sweden from Östersund to Storlien. *Sveriges Geologiska Undersökning* C 774:66.

Gee D. G., Guezou J. C., Roberts D., and Wolff F. C. 1985. The central-southern part of the Scandinavian Caledonides. In *The Caledonide Orogen—Scandinavia and related areas*, edited by Gee D. G. and Stuart B. A. Chichester, New York: John Wiley and Sons Ltd. pp. 109–133.

Gersonde R., Deutsch A., Ivanov B. A., and Kyte F. T. 2002. Oceanic impacts—A growing field of fundamental geoscience. *Deep Sea Research II* 49:951–957.

Grieve R. A. F. 1991, Terrestrial impact: The record in the rocks. *Meteoritics* 26:175–194.

Hampel A., Adam J., and Kukowski N. 2004. Response of the tectonically erosive south Peruvian forearc to subduction of the Nazca Ridge: Analysis of three-dimensional analogue experiments. *Tectonics* 23, doi:10.1029/2003TC001585.

Kenkmann T. and Ivanov B. A. 2006. Target delamination by spallation and ejecta dragging: An example from the Ries crater's periphery. *Earth and Planetary Science Letters* 252:15–29.

Kenkmann T., Hornemann U., and Stöffler D. 2005. Experimental shock synthesis of diamonds in a graphite gneiss. *Meteoritics & Planetary Science* 40:1299–1310.

Kenkmann T., Kiebach F., Eue D., Raschke U., Mittelhaus K., and Pigowske A. 2006. Caledonian deformation overprint onto the Lockne crater, central Sweden: Are resurge gullies real? Workshop on Impact Craters as Indicators for Planetary Environmental Evolution and Astrobiology. pp. 93–94.

Koyi H. 1997. Analogue modelling; From a qualitative to a quantitative technique: A historical outline. *Journal of Petroleum Geology* 20:223–283.

Langenhorst F. and Deutsch A. 1994. Shock experiments on pre-heated α- and ß-quartz: I. Optical and density data. *Earth and Planetary Science Letters* 125:407–420.

Larson S. A., Tullborg E. L., Cederbom C., and Stiberg J. P. 1999.

Sveconorwegian and Caledonian foreland basins in the Baltic Shield revealed by fission-track thermochronology. *Terra Nova* 11:210–215.

Lindqvist J. E. and Andréasson P. G. 1987. Illite crystallinity and prograde metamorphism in thrust zones of the Scandinavian Caledonides. *Science Géologique Bulletin* 40:217–230.

Lindström M. and Sturkell E. F. F. 1992. Geology of the Early Paleozoic Lockne impact structure, central Sweden. *Tectonophysics* 216:169–185.

Lindström M., Simon S., Paul B., and Kessler K. 1983. The Ordovician and its mass movements in the Lockne area near the Caledonian margin, central Sweden. *Geologica et Palaeontologica* 17:17–27.

Lindström M., Ekvall J., Hagenfeldt S. E., Säwe B., and Sturkell E. F. F. 1991. A well-preserved Cambrian impact exposed in central Sweden. *Geologische Rundschau* 80:201–204.

Lindström M., Sturkell E. F. F., Törnberg R., and Ormö J. 1996. The marine impact crater at Lockne, central Sweden. *Geologiska Föreningen i Stockholm Förhandlingar* 118:193–206.

Lindström M., Ormö J., Sturkell E. F. F., and Dalwigk I. von. 2005a. The Lockne crater: Revision and reassessment of structure and impact stratigraphy. In *Impact tectonics*, edited by Koeberl C. and Henkel H. New York: Springer. pp. 357–388.

Lindström M., Shuvalov V. V., and Ivanov B. A. 2005b. Lockne crater as a result of a marine-target oblique impact. *Planetary and Space Science* 53:803–815.

Lohrmann J., Kukowski N., Adam J., and Oncken O. 2003. The impact of analoque material properties on the geometry, kinematics, and dynamics of convergent sand wedges. *Journal of Structural Geology* 25:1691–1711.

Lui J. Y. and Ranalli G. 1992. Stresses in an overtrhrust sheet and propagation of thrusting: An airy stress function solution. *Tectonics* 11:549–559.

McClay K. R. 1992. Glossary of thrust tectonics terms. In *Thrust tectonics*, edited by McClay K. R. London: Chapman and Hall. pp. 419–433.

Middleton M. F., Tullborg E. L., Larson S. A., and Björklund L. 1996. Modelling of a Caledonian foreland basin in Sweden: Petrophysical constraints. *Marine and Petroleum Geology* 13: 407–413.

Mulugeta G. 1988. Modeling the geometry of Coulumb thrust wedges. *Journal of Structural Geology* 10:847–859.

Ormö J. and Lindström M. 2000. When a cosmic impact strikes the sea bed. *Geological Magacine* 137:67–80.

Ormö J. and Miyamoto H. 2002. Computer modelling of the water resurge at a marine impact: The Lockne crater, Sweden. *Deep Sea Research II* 49:983–994.

Ormö J., Shuvalov V. V., and Lindström M. 2002. Numerical modelling for target water depth estimation of marine-target impact craters. *Journal of Geophysical Research* 107:31–39.

Ormö J., Sturkell E. F. F., and Lindström M. 2007. Sedimentary breccias marking the resurge stage of the Lockne and Tvären marine-target impact craters (Sweden). *Meteoritics & Planetary Science* 42. This issue.

Pigowske A., Mittelhaus K., Kiebach F., Eue D., Raschke U., and Kenkmann T. 2006. Preliminary results of a geological mapping project of the western Lockne crater, central Sweden. Workshop on Impact Craters as Indicators for Planetary Environmental Evolution and Astrobiology. pp. 57–58.

Riller U. 2005. Structural characteristics of the Sudbury impact structure, Canada: Impact-induced versus orogenic deformation — A review. *Meteoritics & Planetary Science* 40:1723–1740.

Roberts D. and Gee D. G. 1985. An introduction to the structure of the Scandinavian Caledonides. In *The Caledonide Orogen—Scandinavia and related areas*, edited by Gee D. G. and Stuart B. A. New York: John Wiley and Sons Ltd. pp. 55–68.

Schellart W. P. 2000. Shear test results for cohesion and friction coefficients for different granular materials: Scaling implications for their usage in analogue modeling. *Tectonophysics* 324:1–16.

Simon S. 1987. Stratigraphie, Petrographie und Entstehungsbedingungen von Grobklastika in der autochthonen, ordovizischen Schichtenfolge Jämtlands (Schweden). *Sveriges Geologiska Undersökning* C815:1–156.

Sturkell E. F. F. 1998a. The marine Lockne impact structure, Jämtland, Sweden: A review. *Geologische Rundschau* 87:253–267.

Sturkell E. F. F. 1998b. Impact related Ir anomaly in the Middle Ordovician Lockne impact structure, Jämtland, Sweden. *Geologiska Föreningen i Stockholm Förhandlingar* 120:333–336.

Sturkell E. F. F. and Lindström M. 2004. The target peneplain of the Lockne impact crater. *Meteoritics & Planetary Science* 39:1721–1731.

Sturkell E. F. F., Broman C., Forsberg P., and Torssander P. 1998. Impact-related hydrothermal activity in the Lockne impact structure, Jamtland, Sweden. *European Journal of Mineralogy* 10:589–606.

Shuvalov V. V., Ormö J., and Lindström M. 2005. Hydrocode simulation of the Lockne marine target impact event. In *Impact tectonics*, edited by Koeberl C. and Henkel H. N. New York: Springer. pp. 405–422.

Therriault A. and Lindström M. 1995. Planar deformation features in quartz grains from the resurge deposit of the Lockne crater, Sweden. *Meteoritics* 30:700–703.

Thorslund P. 1940. On the Chasmops Series of Jemtland and Södermanland (Tvären). *Sveriges Geologiska Undersökning* C436:191.

Trepmann C. A. and Spray J. G. 2005. Planar microstructures and Dauphiné twins in shocked quartz from the Charlevoix impact structure, Canada. In *Large meteorite impacts III*, edited by Kenkmann T., Hörz F., and Deutsch A. GSA Special Paper #384. Boulder, Colorado: Geological Society of America. pp. 315–328.

von Dalwigk I. and Ormö J. 2001. Formation of resurge gullies at impacts at sea: The Lockne crater, Sweden. *Meteoritics & Planetary Science* 36:359–369.

Warr L. N., Greiling R. O., and Zachrisson E. 1996. Thrust-related very low grade metamorphism in the marginal part of an orogenic wedge, Scandinavian Caledonides. *Tectonics* 15:1213–1229.

Wickman F. E. 1988. Possible impact structures in Sweden. In *Deep drilling in crystalline bedrock, I. The deep gas drilling in the Siljan impact structure, Sweden and astroblemes*, edited by Boden A. and Eriksson K. G. Berlin: Springer-Verlag. pp. 298–327.

Willett S. D. 1992. Dynamic and kinematic growth and change of a Coulomb wedge. In *Thrust tectonics*, edited by McClay K. R. London: Chapman and Hall. pp. 19–31.